Analyst

Accepted Manuscript

ROYAL SOCIETY OF CHEMISTRY

www.rsc.org/analyst

A colorimetric method of analysis for trace amounts of hydrogen peroxide with the use of the nano–properties of Molybdenum disulfide

Xinrong Guo,[a] Yong Wang,[a] Fangying Wu,[a] Yongnian Ni,[a,b,*] and Serge Kokot[c]

[a] *College of Chemistry, Nanchang University, Nanchang 330031, China*

[b] *State Key Laboratory of Food Science and Technology, Nanchang University, Nanchang 330047, China*

[c] *School of Chemistry, Physics and Mechanical Engineering, Science and Engineering Faculty, Queensland University of technology, Brisbane 4001, Australia*

* Corresponding author. Address: Department of Chemistry, Nanchang University, Nanchang 330031, China. Tel./fax: 86 791 3969500. E–mail address: ynni@ncu.edu.cn (Y. N. Ni); s.kokot@qut.edu.au (S. Kokot)

Abstract

Molybdenum disulfide (MoS_2) is an emerging material with some unique physical and electronic properties somewhat comparable to those of graphene. It was made with the use of a simple hydrothermal process, and has a layered structure similar to that of graphene. Also, it has peroxidase–like catalytic activity and is able to catalyze the oxidation of colorless peroxidase substrate, 3,3',5,5'–tetramethylbenzidine (TMB), in the presence of H_2O_2 to produce a blue product. This reaction used MoS_2 as a useful peroxidase, which involved a colorimetric method for trace analysis of H_2O_2 in water, e.g. lake waters. This method is uncomplicated, inexpensive and highly sensitive for H_2O_2 in the 0.125 – 1.75 μM range (LOD: 0.08 μM). It is also quite stable in the presence of many common inorganic and organic potentially interfering compounds, e.g. metal ions as well as amino - acids and sugars.

Keywords: Molybdenum disulfide; Hydrogen peroxide analysis; 3,3',5,5'–tetramethylbenzidine (TMB); Colorimetric method.

1. Introduction

Two-dimensional (2D) materials, such as graphene and transition metal dichalcogenides (TMDCs), have unique electronic, optical and mechanical properties.[1–3] Graphene has a single layer graphite structure, which has a large specific surface area, useful electronic and mechanical properties, and as a result, it has been widely applied in many research studies,[4] e.g. as a co–catalyst in photo–catalysis of the hydrogen evolution reaction (HER). Also, molybdenum disulfide (MoS_2) with exposed edges has been recently reported as a promising electro–catalyst for the HER,[5] e.g. as a nano–tungsten carbide attached to graphene on a MoS_2 layer.[6] Additionally, the layered TMDC's cations have been used in a similar way,[2,3] e.g. as solid lubricants,[7] batteries[8] and catalysts.[9]

MoS_2 is one of the layered TMDC materials, which has a layered structure similar to that of graphene. It is composed of Mo–S–Mo groups, which are held together by weak van der Waals forces.[10-12] Preparative methods for mono– and multi–layered MoS_2 have been described, and include mechanical exfoliation, lithium intercalation and exfoliation, liquid phase exfoliation and chemical vapor deposition.[1] A mono–layer of MoS_2 is a semiconductor, which is potentially suitable for making sensors, transistors, optoelectronics and electroluminescent devices. It has a direct band gap and high mobility in contrast to the multilayered MoS_2, which has an indirect band gap.[13] Compared to graphene, MoS_2 has attracted attention because of its unique physical properties, especially its complementary electronic behavior. Also, MoS_2 has been used as a solid lubricant in industry,[14] and it is a well-known catalyst for the production of hydrogen gas.[10,15] When MoS_2 is used as a co–catalyst with semiconductors such as TiO_2,[5] CdS[9] and g–C_3N_4,[16] it enhances significantly the production of H_2 and the degradation of some pollutants.[17]

Hydrogen peroxide (H_2O_2) plays an important role in many enzymatic reactions, as well as in essential biological processes such as the metabolism of proteins and carbohydrates or in the immune response process.[18] Consequently, an uncomplicated, inexpensive, rapid and sensitive analytical method for H_2O_2 would be particularly welcome because it could be used for bio–assays, in chemical and pharmaceutical industries as well as in food security and environmental applications.[19–23] In this context, several biochemical methods for monitoring H_2O_2 in blood have been developed, especially with the use of biosensors.[24] Other analytical methods for the analysis of this substance have been reported, including fluorescence,[25] cell imaging,[26] electrochemical[14] and colorimetric assays.[27] The colorimetric methods have been the ones, which fulfilled the above method criteria and consequently, such methods even now are important for bio–analysis

of H_2O_2. Many currently available colorimetric methods for the analysis of this analyte usually use peroxidase enzymes to catalyze the suitable enzymatic chromogenic substrate, TMB, to produce a blue product. An example of one such method commonly uses horseradish peroxidase (HRP).[28] However, these natural enzyme based methods generally need time–consuming and expensive preparation procedures, as well as analyte purification and strict storage conditions.[27] The use of nano–materials as efficient peroxidase mimetics are well known and include polypyrrole,[27] Fe_2O_3–graphene,[29] CuS,[30] $ZnFe_2O_4$,[31] FeS and FeSe.[32] ultra–small MoS_2 nanoparticles,[14] hemin–MoS_2 nanosheets,[33] carbon nanodots[34] and tungsten carbide nanorods.[35] The nanoparticle approach has gained traction in its application because the nanoparticles are cost–effective, easily obtained, relatively stable to biodegradation, and less vulnerable to denaturation.[32] Although electrochemical detection of H_2O_2 based on MoS_2 has been reported,[14,36] such biosensors are limited by the lack of an ideal approach for immobilization of the enzymes on an electrode surface.[37]

Hence, the aims of this work were: (1) to synthesise MoS_2 and investigate its properties when peroxidase substrate TMB and H_2O_2 co–existed; (2) to use the MoS_2 as a catalyst for quantitative analysis of H_2O_2 based on a colorimetric method and research its catalytic mechanism, and (3) to apply this new and simple method to analyse the H_2O_2 in lake waters.

2. Experimental

2.1. Chemicals and materials

Sodium molybdate dihydrate ($Na_2MoO_4{\cdot}2H_2O$) and L–cysteine were purchased from Shanghai Chemical Reagent Co., Ltd. 3,3',5,5'–tetramethylbenzidine (TMB) and amino acids were purchased from Shanghai Sangon Biotech Co., Ltd. TMB was stored in a refrigerator at 4 °C. H_2O_2 (30%), HCl (12 M) and terephthalic acid (TA) were purchased from Shanghai Sinopharm Chemical Reagent Co., Ltd. All the reagents and chemicals were Analytical Grade reagents and were used without further purification. The stored TMB (1.0 mM) solution was prepared by dissolving crystalline TMB (0.06 mg) in 50 mL 0.02 M HCl and then diluted to 250 mL with 0.02 M HCl. MoS_2 (0.1 mg mL^{-1}) was prepared by dissolving 10.0 mg synthesized MoS_2 in 50 mL water and diluted to 100 mL. This solution was generally stable for two months at room temperature (20 °C). All the glassware were soaked in aqua–regia and thoroughly rinsed with doubly distilled water three times before use. The double-distilled water was used throughout this work.

2.2. Apparatus

Absorbance measurements were carried out on an Agilent 8453 UV–vis spectrophotometer (Agilent Technologies, Santa Clara, CA, USA). The scanning electron microscopy (SEM) images were made on a JSM–6701F microscope system (JEOL Co., Tokyo, Japan). Transmission electron microscopy (TEM) and energy dispersive X–ray spectroscopy (EDS), for measuring the structure and morphology of the resulting compounds, were carried out with the use of a JEM–2010 (JEOL Co., Japan), and the associated point and linear resolutions were found to be 0.23 nm and 0.14 nm, respectively. The accelerating voltage was set at 200 kV. The sample was placed on a carbon–coated copper grid by depositing a drop of the test solution on the grid. It was dried in air at room temperature. X–ray photoelectron spectroscopy (XPS) was performed on an ESCALAB 250Xi Microprobe (Thermo Scientific, USA) using 200 W mono–chromated Al Kα radiation. X–ray diffraction (XRD) spectra were recorded with a Bede D1 high–resolution X–ray diffractometer system (Bede Co., UK). The fluorescence measurements were made on a Hitachi fluorescence spectrophotometer F–7000 (Hitachi Ltd., Tokyo, Japan).

2.3. Synthesis of MoS_2

The layered MoS_2 was prepared by a hydrothermal synthesis.[4,38] $NaMoO_4 \cdot 2\ H_2O$ (0.25 g) was dissolved in 25 mL water and 0.1 M HCl was added to this solution to adjust the pH to 6.5. Then, 0.5 g L^{-1} L-cysteine and 75 mL water were added to the solution, which was then ultra–sonicated for 10 min. The mixture was transferred to a Teflon–lined, stainless steel autoclave (100 mL) and treated for 36 h at 200 °C. The mixture was allowed to cool and the black precipitate was collected by centrifugation (12000 rpm for 30 min). The black precipitate was then thoroughly washed several times with water, and vacuum dried at 80 °C for 24 h.

2.4. Peroxidase–like activity measurements

The peroxidase–like catalytic properties of MoS_2 were investigated by oxidizing the peroxidase substrate, TMB, in the presence of H_2O_2, and the formation of the blue product was tested. The control experiments were performed in the absence of H_2O_2 or MoS_2 in the presence of the mixture, which contained 1.0 mM TMB (0.9 mL) and 0.1 M pH 4.0 acetate buffer (1.0 mL). The catalytic oxidation of TMB by MoS_2 (0.1 mg mL^{-1}, 20 μL) in the presence of H_2O_2 (1.0 mM, 80 μL) was also determined under the conditions described

above; the absorbance change during each reaction above was recorded at 652 nm after 40 min.

2.5. Procedure for colorimetric analysis of H_2O_2

The procedure for the colorimetric analysis of H_2O_2 was started by the addition of different concentrations of H_2O_2 into 0.1 M pH 4.0 acetate buffer solutions (1.0 mL) in the presence of 1.0 mM TMB (0.9 mL) and 0.1mg mL^{-1} MoS_2 (20 μL). Afterwards, the colorimetric reactions of the mixed solutions were heated at 30 °C on a water bath with stirring for 40 min. were completed. Afterwards, the absorbance of each mixed solution was used for the analysis at 652 nm. The final concentrations of H_2O_2 in the system varied from 0.125 to 1.75 μM.

2.6. Analysis of H_2O_2 in aqueous samples

H_2O_2 was previously analysed in rain water and other different water samples,[39–41] and in this work , we verified the capability of the new peroxidase–like reagent, MoS_2 for the detection of H_2O_2 in the water samples. These were collected from the Qianhu Lake, Nanchang University, and the collected sample was spiked with H_2O_2. After standing for 5 h, the water samples (about 300 mL) were filtered three times to remove any solid impurities, and the filtrate was centrifuged at 12000 rpm for 15 min to remove most of the microorganisms. Then, the water samples were diluted with the acetate buffer (0.1 M, pH 4.0), and spiked with H_2O_2 at different concentrations. In the presence of 20.0 μL MoS_2 (0.1 mg mL^{-1}), the 0.9 mL TMB (1.0 mM) was added to the water samples (1.0 mL) obtained above. These samples were diluted to 2.0 mL with water. Each sample was heated with stirring for 40 min at 30 °C on a water bath, and then their absorbance values were measured at 652 nm.

3. Results and discussion

3.1. Characterization of the MoS_2

MoS_2 was prepared by a hydrothermal process (Section of 2.3).[4,38] Thus, MoS_2 was successfully synthesized in the solution-phase where Na_2MoO_4 was reduced to MoS_2 by L–cysteine, which acted as the sulfide source as well as the reducing agent. It released H_2S during the hydrothermal process (Eqn. 1 and 2 below, and Scheme 1A):

$$HSCH_2CHNH_2COOH + H_2O \rightarrow CH_3COCOOH + NH_3 + H_2S \quad (1)$$

$$4\ MoO_4^{2-} + 9\ H_2S + 6\ CH_3COCOOH \rightarrow 4\ MoS_2 + SO_4^{2-} + 6\ CH_3COCOO^- + 12\ H_2O \quad (2)$$

The structure and morphology of the synthesized MoS_2 were investigated with the use of XRD, SEM, TEM, EDS and XPS. XRD intensity plots of MoS_2 (Fig. 1A) showed a weak broad feature, which could be attributed to low crystallinity in the sample. Additionally, there were three diffraction peaks at (002), (100), (110) corresponding to 15.1°, 34.2° and 58.5°, respectively. The weak diffraction peak (002), suggested that the MoS_2 layers were stacked along the *c* axis. EDS of the MoS_2 (Fig. 1B) confirmed the presence of C, O, Mo and S, and the corresponding SEM images (Fig. 1C) suggested that the different MoS_2 layers were folded and tangled forming a multilayer morphology. Also, interconnected ripples and corrugations were clearly present, and they are consistent with the ready flexibility of the MoS_2 planes, thus producing structural deformation.[42] TEM images of MoS_2 (Fig. 1D) effectively supported the SEM observations. They revealed MoS_2 structures which displayed well–defined plate-like morphology, which was composed of large–scale, tightly stacked thin layers.

The XPS spectrum of MoS_2 (Fig. 1E) displayed the Mo and S elemental peaks as well as those of the Na, N, C and O elements, which confirmed the presence of the compounds involved in the hydrothermal synthesis. High–resolution XPS spectra for Mo 3d and S 2p were also collected (Figs. 1F and 1G), respectively. The Mo3d spectrum was deconvoluted into five single peaks; two peaks, located at 228.91 and 232.10 eV, were attributed to the binding energies of the Mo $3d_{5/2}$ and Mo $3d_{3/2}$ doublet peaks, respectively. The peaks were typical of the Mo^{4+} oxidation state in MoS_2, while the remaining peak at 226.22 eV corresponded well to the S 2s lines of MoS_2.[38,43] In contrast, the S 2p region could be explained by the three 2 $p_{3/2}$ – 2 $p_{1/2}$ spin-orbit doublets (Fig. 1G). The two peaks located at 161.8 and 163.15 eV could be assigned to the binding energies of the 2 $p_{3/2}$ and 2 $p_{1/2}$ lines of MoS_2 in the three S 2p doublets,[43] but the S 2p peaks, located at 161.8 eV, were consistent with the S^{2-} oxidation state of sulfur.[44] Whereas, the peaks for S $2p_{3/2}$ and 2 $p_{1/2}$ at 162.58 and 164.40 eV were probably indicative of a bridging S_2^{2-} or poly-sulfides, S_n^{2-}, which formed from the unsaturated S atoms.[45] The high–energy S 2p doublets, with the associated 168.02 eV ($2p_{3/2}$) and 169.4 eV (2 $p_{1/2}$) values, could be attributed to the $S_2O_3^{2-}$ group.[38] The stoichiometric ratio between Mo and S estimated from the quantitative analysis of the Mo $3d_{5/2}$ and S 2s peak intensities of the XPS spectra was close to 1:2; this result further confirmed the formation of MoS_2.

3.2. Peroxidase–like activity of MoS_2

The peroxidase–like activity of MoS_2 was investigated by studying the catalysis of the oxidation of the peroxidase substrate, TMB, in the presence of H_2O_2. Under acidic conditions, although the colorless solution of TMB was slowly oxidised by H_2O_2, it could only be rapidly oxidised to produce the blue colored product in the presence of the peroxidase–like action of the MoS_2 and H_2O_2. This blue product was the charge-transfer complex of the parent diamine and the diimine oxidation products, and it produced two absorption maxima at 370 nm and 652 nm (see Scheme 1B).[46] The UV–vis spectra did not discriminate between three of the four spectra (Fig. 2). Thus, TMB, TMB–H_2O_2 and TMB–MoS_2 systems did not have any well–developed absorption peaks in the 500 to 800 nm range, while MoS_2-TMB-H_2O_2 system showed a strong absorption peak at 652nm; this was the typical peak of the oxidation products of TMB. Images of the different TMB solutions are displayed in the inset, Fig. 2. Thus, the TMB solution remained effectively colorless when either MoS_2 or H_2O_2 was present, i.e. no oxidation reaction occurred. However, this solution turned blue if both H_2O_2 and the MoS_2 were added. These results indicated that MoS_2 showed peroxidase–like activity and effectively catalyzed the oxidation of TMB by H_2O_2 in an acetate buffer.

3.3. Optimization of experimental conditions

The reaction conditions were optimized to establish the appropriate analytical conditions (Fig. S1, Supplementary Information). The effect of reaction time on the catalytic activity of MoS_2 was investigated in the range of 10–70 min. Thus, the catalytic activity of MoS_2 increased with increasing reaction time from 10 min to 30 min (Fig. S1A). Then, the activity increase slowed and effectively stabilised from 30 min to 70 min. As a result 40 min was selected as the optimum reaction time. The effect of MoS_2 concentration in the 0.25 – 3.75 μg mL^{-1} range (Fig. S1B), showed that the catalytic activity of the MoS_2 increased with the MoS_2 concentration up to 1.5 μg mL^{-1}; above this concentration the catalytic activity decreased. In general, the experimental results indicated that the catalytic activity of the MoS_2 differed only slightly between 1.0 μg mL^{-1} and 1.5 μg mL^{-1}. Consequently, 1.0 μg mL^{-1} MoS_2 was chosen for further experiments.

The effect of temperature was studied from 20 to 60 °C (Fig. S1C) and showed that the catalytic activity of MoS_2 increased with increasing temperature from 20 to 30 °C, but after this point, it decreased. Hence, 30 °C was chosen as the experimental temperature.

In the case of pH, the literature suggested that peroxidase–like activity for the catalysis of the oxidation of TMB by H_2O_2 was much higher in acidic than neutral or basic solutions.[29,30] Thus, the acetate buffer was chosen as the optimum reaction medium for the reaction discussed above.

3.4. Mechanism of peroxidase–like activity of MoS_2

In the presence of H_2O_2, MoS_2 could catalyze the oxidation of TMB. Initially, during this reaction process some H_2O_2 decomposes into the ·OH radicals and then, these will oxidize TMB so as to generate the corresponding blue oxidation product. To confirm this outcome, terephthalic acid (TA) was used as a fluorescent probe in the MoS_2–H_2O_2 system. Although TA does not fluoresce itself, on reaction with the ·OH radical, a strongly fluorescent compound, 2–hydroxy terephthalic acid (HTA) forms. The corresponding chemical equation is:[47]

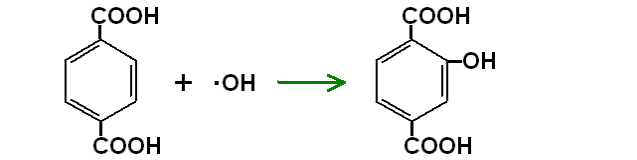

Terephthalic acid **2-hydroxy terephthalic acid**

Subsequently, each of the following solutions – (a) 1.0 μg mL^{-1} MoS_2 without H_2O_2; (b) 50 mM H_2O_2 without MoS_2; (c) 1.0 μg mL^{-1} MoS_2 and 50 mM H_2O_2 was treated with 0.45 mM terephthalic acid and heated in 1mL 0.1 M acetate buffer (pH 4.0) at 30 °C for 12 h. A fluorescence spectrum of each solution was recorded at the excitation wavelength of 324 nm in the range of 300 – 600 nm (Fig. 3). These results showed that with sample (a) no fluorescence was recorded, with sample (b) a very small amount of fluorescence was emitted, but with sample (c) when MoS_2 was added to the solution containing TA and H_2O_2, a strong fluorescence band was observed, i.e. enough of the ·OH radicals were produced to react with the non–luminescent TA to obtain the highly fluorescent HTA. These results strongly suggested that MoS_2 could decompose H_2O_2 to generate the ·OH radicals. This reaction was most likely to occur by the following mechanism: at first H_2O_2 molecules were absorbed on the surface of the MoS_2 and then they were activated by the bound Mo^{4+} to generate the ·OH radicals. These radicals were then stabilized by the MoS_2 via a reaction process involving a partial electron exchange interaction.[48]

3.5. Detection of H_2O_2 based on MoS_2

An analytical method for H_2O_2 in aqueous media was designed on the basis of the optimal experimental conditions discussed in the previous Sections. Thus, measured aliquots of H_2O_2 at different concentrations were added to the acetate buffer solution (pH 4.0), which contained the TMB and MoS_2. The different samples so produced were analyzed with the use of UV–vis absorption spectroscopy (Fig. 4), and the results (inset, Fig. 4) indicated that the absorbance *versus* H_2O_2 concentration calibration plot at 652 nm was linear in the range of 0.125–1.75 μM. The regression equation was $\Delta A = 0.0793\ [H_2O_2]\ (\mu M) + 0.0338$, correlation coefficient was 99.8% (n = 3), and the limit of detection (LOD) for H_2O_2 was 0.08 μM. These results were compared with those from previous methods for analysis of H_2O_2 (Table 1). Importantly, the colorimetric method involving the MoS_2, which mimicked the activity of the peroxidase, recorded the lowest range value, the lowest LOD and a convenient working temperature (30 ^oC). It should be noted that higher range values are of lesser importance because the sample can always be diluted. Thus, the mimic peroxidase compares well with the best 3–4 other peroxidase nano-mimetic substances,[28,49,50] and is arguably the best performer of the three measured variables (Table 1). Importantly, when the results from this work were compared with other kinds of layered MoS_2[54] systems for the detection of H_2O_2, they showed a lower limit of detection, and this result suggested that the novel peroxidase–like reagent (MoS_2) showed better sensitivity and selectivity for the analysis of trace amounts of H_2O_2.

The new peroxidase–like reagent, MoS_2, was also tested on H_2O_2 spiked water samples (Table 2), and the recovery results were in the range of 94.9–107.2% (average: 99.3%) for three repeat samples. The relative standard deviation (RSD) values were in the range of 5.5–11.2% (average: 8.1%). Based on these results, the layer MoS_2 was able to analyse trace amounts of H_2O_2 in water samples, and can be regarded as a new substance , which mimiced peroxidase activity.

3.6. Potentially interfering substances

In natural samples, there are often organic and/or inorganic substances, which may or may not interfere with the analysis of H_2O_2 with the use of the novel MoS_2 layer method. Consequently, a large number of potentially interfering metal and non-metal ions as well as common organic compounds were tested in different amounts. These substances included: common metal and non–metal cations – K^+, NH_4^+, Ca^{2+}, Mg^{2+}, Zn^{2+}, Ni^{2+}, Ba^{2+} and Al^{3+} (all 10 mM), as well as organic compounds: glucose, fructose, sucrose, lactose, and

various amino acids - aspartic acid (Asp), methionine (Met), phenylalanine (Phe), isoleucine (Ile), proline (Pro), glycine (Gly), arginine (Arg), valine (Val), tryptophan (Trp), glutamate (Glu), leucine (Leu), histidine (His), serine (Ser) and alanine (Ala) (all 50 mM). The effect of each of the potential interfering compound was reflected in the bar graph (Fig. S2); each bar represented the concentration of H_2O_2 (2.0×10^{-6} mol L^{-1}) in the presence of an interfering substance and the results were represented as normalized spectral intensities $(A–A_0)/A$. In general, compared with the H_2O_2 concentration without any interferents, there was only a small interference effect observed in the presence of an interferent. The relative error was less than 5% in all cases.

4. Conclusions

MoS_2 with its graphene–like layered structure was successfully synthesized with the use of an environmentally effective and uncomplicated hydrothermal method. In so doing, it was found that the layered MoS_2 had peroxidase–like, catalytic reactivity. The behavior of the MoS_2 was dependent on time, pH and temperature similar to that noted for the peroxidase–like substances. Hence, MoS_2 could catalyze the oxidation of peroxidase substrate, TMB, with H_2O_2 to give a blue molecular product. It was found that the peak maximum at 652 nm corresponding to the above blue substance produced a linear absorption *versus* concentration plot, and this formed the basis for the colorimetric method for the detection of H_2O_2 in the 0.125–1.75 μM range. The average %Recovery and %RSD values were 99.3% and 8.1%, respectively. Importantly, the analytical performance of this novel method, which mimicked peroxidase, was compared with several other peroxidase nanomimetics for the analysis of H_2O_2 on the basis of three key experimental variables – lowest Range value, LOD and Temperature. It arguably performed better. Also, this novel method involving the MoS_2, will be particularly suitable for the analysis of natural waters as well as for environmental and bio–chemical samples.

Acknowledgements

The authors gratefully acknowledge the financial support of this study by the National Natural Science Foundation of China (NSFC–21365014 and NSFC–21305061), the Natural Science Foundation of Jiangxi Province (20132BAB213011 and 20132BAB203011), the Education Department Science Foundation of Jiangxi Province (GJJ13026), and the State Key Laboratory of Food Science and Technology of Nanchang

University (SKLF–ZZA201302 and SKLF–ZZB201303).

References

1 X. Huang, Z. Y. Zeng and H. Zhang, *Chem. Soc. Rev*., **2013**, 42, 1934–1946.

2 Q. H. Wang, K. Kalantar-Zadeh, A. Kis, J. N. Coleman and M. S. Strano, *Nat. Nanotechnol*., **2012**, 7, 699–712.

3 K. S. Novoselov, A. K. Geim, S. V. Morozov, D. Jiang, Y. Zhang, S. V. Dubonos, I. V. Grigorieva and A. A. Firsov, *Science*, **2004**, 306, 666–669.

4 K. Chang and W. X. Chen, *ACS Nano,* **2011**, 5(6), 4720–4728.

5 Q. J. Xiang, J. G. Yu, M. Jaroniec, *J. Am. Chem. Soc*., **2012**, 134, 6575–6578.

6 Y. Yan, B. Y. Xia, X. Y. Qi, H. B. Wang, R. Xu, J. Y. Wang, H. Zhang, X. Wang, *Chem. Commun*., **2013**, 49, 4884–4886.

7 M. S. Whittingham, *Chem. Rev*., **2004**, 104, 4271–4302.

8 L. Rapoport, N. Fleischer and R. Tenne, *J. Mater. Chem*., **2005**, 15, 1782–1788.

9 T. T. Jia, A. Kolpin, C. S. Ma, R. C. T. Chan, W. M. Kwok and S. C. E. Tsang, *Chem. Commun*., **2014**, 50, 1185–1188.

10 T. F. Jaramillo, J. P. Jorgensen, J. Bonde, J. H. Nielsen, S. Horch and I. Chorkendorff, *Science,* **2007**, 317, 100–102.

11 Z. Y. Zeng, Z. Y. Yin, X. Huang, H. Li, Q. Y. He, G. Lu, F. Boey and H. Zhang, *Angew. Chem. Int. Ed*., **2011**, 50, 11093–11097.

12 H. S. S. R. Matte, A. Gomathi, A. K. Manna, D. J. Late, R. Datta, S. K. Pati and C. N. R. Rao, *Angew. Chem. Int. Ed*., **2010**, 49, 4059–4062.

13 Z. H. Tang, Q. Y. Wei and B. C. Guo, *Chem. Commun*., **2014**, 50, 3934–3937.

14 T. Y. Wang, H. C. Zhu, J. Q. Zhuo, Z. W. Zhu, P. Papakonstantinou, G. Lubarsky, J. Lin and M. X. Li, ,*Anal. Chem*., **2013**, 85, 10289–10295.

15 Y. G. Li, H. L. Wang, L. M. Xie, Y. Y. Liang, G. S. Hong and H. J. Dai, *J. Am. Chem. Soc*., **2011**, 133, 7296–7299.

16 L. Ge, C. C. Han, X. L. Xiao and L. L. Guo, *Int. J. Hydrogen Energy*, **2013**, 38, 6960-6969.

17 Y. L. Min, G. Q. He, Q. J. Xu and Y. C. Chen, *J. Mater. Chem. A*, **2014**, 2, 2578–2584.

18 P. Wentworth Jr., L. H. Jones, A. D. Wentworth, X. Y. Zhu, N. A. Larsen, I. A. Wilson, X. Xu, W. A. Goddard III, K. D. Janda, A. Eschenmoser and R. A. Lerner, *Science*, **2001**, 293, 1806–1811.

19 H. Jin, D. A. Heller, M. Kalbacova, J. H. Kim, J. Q. Zhang, A. A. Boghossian, N. Maheshri and M. S. Strano, *Nat. Nanotechnol*., **2010**, 5, 302–309.

20 X. Q. Chen, X. Z. Tian, I. Shin and J. Y. Yoon, *Chem. Soc. Rev*., **2011**, 40, 4783–4804.

21 X. H. Shu, Y. Chen, H. Y. Yuan, S. F. Gao and D. Xiao, *Anal. Chem*., **2007**, 79, 3695–3702.

22 Y. Hitomi, T. Takeyasu and M. Kodera, *Chem. Commun*., **2013**, 49, 9929–9931.

23 Y. W. Zhang, J. Q. Tian, S. Liu, L. Wang, X. Y. Qin, W. B. Lu, G. H. Chang, Y. L. Luo, A. M. Asiri, A. O. Al-Youbi and X. P. Sun, *Analyst*, **2012**, 137, 1325–1328.

24 V. Thome-Duret, G. Reach, M. N. Gangnerau, F. Lemonnier, J. C. Klein, Y. N. Zhang, Y. B. Hu and G. S. Wilson, *Anal. Chem*., **1996**, 68, 3822–3826.

25 V. V. Belousov, A. F. Fradkov, K. A. Lukyanov, D. B. Staroverov, K. S. Shakhbazov, A. V. Terskikh and S. Lukyanov, *Nat. Methods*, **2006**, 3, 281–286.

26 Y. H. A. Liu and X. B. Liao, *Curr. Org. Chem*., **2013**, 17, 654–669.

27 Y. Tao, E. G. Ju, J. S. Ren and X. G. Qu, *Chem. Commun*., **2014**, 50, 3030–3032.

28 Y. J. Guo, J. Li and S. J. Dong, *Sens. Actuators B Chem*., **2011**, 160, 295–300.

29 Z. X. Xing, J. Q. Tian, A. M. Asiri, A. H. Qusti, A. O. Al–Youbi and X. P. Sun, *Biosens. Bioelectron*., **2014**, 52, 452–457.

30 A. K. Dutta, S. Das, S. Samanta, P. K. Samanta, B. Adhikary and P. Biswas, *Talanta*, **2013**, 107, 361–367.

31 L. Su, J. Feng, X. M. Zhou, C. L. Ren, H. H. Li and X. G. Chen, *Anal. Chem*., **2012**, 84, 5753–5758.

32 A. K. Dutta, S. K. Maji, D. N. Srivastava, A. Mondal, P. Biswas, P. Paul and B. Adhikary, *ACS Appl. Mater. Interfaces*, **2012**, 4, 1919–1927.

33 B. L. Li, H. Q. Luo, J. L. Lei and N. B. Li, *RSC Adv*., **2014**, 4, 24256–24262.

34 W. B. Shi, Q. L. Wang, Y. J. Long, Z. L. Cheng, S H. Chen, H. Z. Zheng and Y. M. Huang, *Chem. Commun.*, **2011**, 47, 6695–6697.

35 N. Li, Y. Yan, B. Y. Xia, J. Y. Wang and X. Wang, *Biosens. Bioelectron*., **2014**, 54, 521–527.

36 H. Y. Song, Y. N. Ni and S. Kokot, *Biosens. Bioelectron.*, **2014**, 56, 137–143.

37 L. Wang and E. K. Wang, *Electrochem. Commun*., **2004**, 6, 225–229.

38 Y. Wang and Y. N. Ni, *Anal. Chem.*, **2014**, 86, 7463–7470.

39 H. Heli and J. Pishahang, *Electrochimica Acta*., **2014**, 123, 518-526.

40 H. Heli, N. Sattarahmady, R. D. Vais and A. R. Mehdizadeh, *Sens. Actuators B*, **2014**, 192, 310–316.

41 S. H. He, W. B. Shi, X. D. Zhang, J. Li and Y. M. Huang, *Talanta*, **2010**, 82, 377–383.

42 X. L. Li and Y. D. Li, *J. Phys. Chem. B*, **2004**, 109, 13893–13900.

43 Y. Yan, B. Y. Xia, X. M, Ge, Z. L. Liu, J. Y. Wang and X. Wang, *ACS Appl. Mater. Interfaces*, **2013**, 5, 12794–12798.

44 B. L. Li, L. X. Chen, H. L. Zou, L. L. Jing, H. Q. Luo and N. B. Li, *Nanoscale*, **2014**, 6, 9831–9838.

45 H. Vrubel, D. Merki and X. Hu, *Energy Environ. Sci*., **2012**, 5, 6136–6144.

46 P. D. Josephy, T. Eling and R. P. Mason, *J. Biol. Chem.*, **1982**, 257, 3669–3675.

47 K. Ishibashi, A. Fujishima, T. Watanabe and K. J. Hashimoto, *Photochem. Photobiol. A*, **2000**, 134, 139–142.

48 W. B. Shi, X. D. Zhang, S. H. He and Y. M. Huang, *Chem. Commun*., **2011**, 47, 10785-10787.

49 M. Liu, B. X. Li, X. Cui, *Talanta*, **2013**, 115, 837–841.

50 Z. S. Wu, S. B. Zhang, M. M. Guo, C. R. Chen, G. L. Shen and R. Q. Yu, *Anal. Chim. Acta*, **2007**, 584, 122–128.

51 L. J. Chen, B. Sun, X. D. Wang, F. M. Qiao and S. Y. Ai, *J. Mater. Chem. B*, **2013**, 1, 2268–2274.

52 X. N. Hu, A. Saran, S. Hou, T. Wen, Y. L. Ji, W. Q. Liu, H. Zhang, W. W. He, J. J. Yin and X. C. Wu, *RSC Adv*., **2013**, 3, 6095–6105.

53 Y. Liu, M. Yuan, L. J. Qiao and R. Guo, *Biosens. Bioelectron*., **2014**, 52, 391–396.

54 T. R. Lin, L. S. Zhong, L. Q. Guo, F. F. Fu and G. N. Chen, *Nanoscale*, **2014**, 6, 11856–11862.

Captions

Scheme 1. (A) Preparation of MoS_2 with the use of a simple hydrothermal method, **(B)** A stepwise demonstration of the highly–efficient peroxidase–like activity of MoS_2 for the detection of H_2O_2.

Figure 1. (A) XRD results for MoS_2. **(B)** EDS of MoS_2. **(C)** SEM image of MoS_2. **(D)** TEM image of MoS_2 (**Inset B** – a high–resolution TEM image of MoS_2 (scale: 20 nm)). **(E)** XPS survey spectrum of MoS_2. **(F)** High–resolution peak–fitting XPS spectra of the Mo 3d regions for MoS_2. **(G)** High–resolution peak–fitting XPS spectra of the S 2p regions for MoS_2.

Figure 2. UV–vis spectral changes at 652 nm corresponding to: **(a)** TMB, **(b)** TMB–MoS_2, **(c)** TMB–H_2O_2 and **(d)** TMB–H_2O_2–MoS_2, in pH 4.0 acetate buffer (0.1 M) at 30 °C for 40 min. **Inset:** images of different reaction systems: (a), (b), (c) and (d).

Figure 3. Effect of the MoS_2 on the formation of the hydroxyl radical using terephthalic acid as a fluorescent probe: **(a)** 1.0 μg mL^{-1} MoS_2 without H_2O_2; **(b)** 50 mM H_2O_2 without MoS_2; **(c)** 1.0 μg mL^{-1} MoS_2 and 50 mM H_2O_2. Reaction conditions: 0.45 mM terephthalic acid; the different solutions were incubated in 0.1 M acetate buffer (pH 4.0) at 30 °C for 12 h.

Figure 4. UV–vis absorption spectra changes at 652 nm of H_2O_2 in the TMB–MoS_2 system at different concentrations. Reaction conditions: 0.45 mM TMB and 1.0 μg mL^{-1} MoS_2 were reacted in 0.1 M acetate buffer (pH 4.0) at 30 °C for 40 min. **Inset:** Calibration plot for the analysis of H_2O_2 with use of the TMB–MoS_2 system. Standard deviation error bars were estimated from three measurements.

Table 1

Comparison of performance of the MoS_2 as a mimic peroxidase for the determination of trace amounts of H_2O_2 with that of other biosensors

Catalysts used	Ranges (μM)	LOD (μM)	Temperature (°C)	Refs.
PTEBS	1.0 – 10.0	0.3	45	49
Gold nanoparticles (GNPs)	1.3 – 41.0	0.6	25	50
2D ultrathin nanosheets of Co/Al	10.0 – 200.0	10.0	25	51
Au@Pt NRs	10.0 – 1000	8.9	37	52
Fe_2O_3–graphene nanostructures	0.2 – 10.0	0.5	45	28
Protein–Fe_3O_4 complex	0.5 – 200	0.2	35	53
MoS_2 nanosheets	5.0 – 100	1.5	30	54
Layered MoS_2	0.125 – 1.75	0.08	30	this work

Table 2

Analysis of hydrogen peroxide (μM) in spiked water samples (n = 3)

Samples [a]	Detected	Added	Found	Recovery (%)	RSD (%)
#1	ND [b]	0.50	0.47	94.9	11.2
#2	ND	1.0	0.95	95.8	5.5
#3	ND	1.5	1.60	107.2	7.7

[a] Water samples were collected from the Qianhu lake on the Nanchang University campus, and spiked at three different concentration levels.

[b] Not detected.

Scheme 1

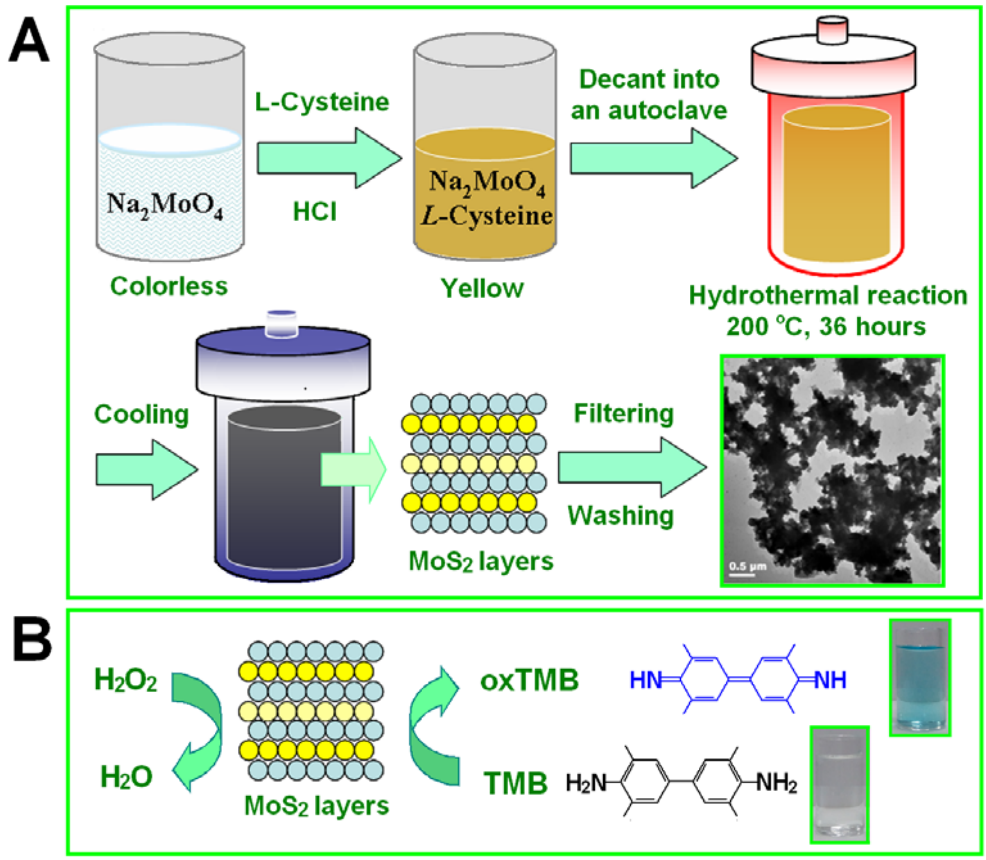

Figure 1

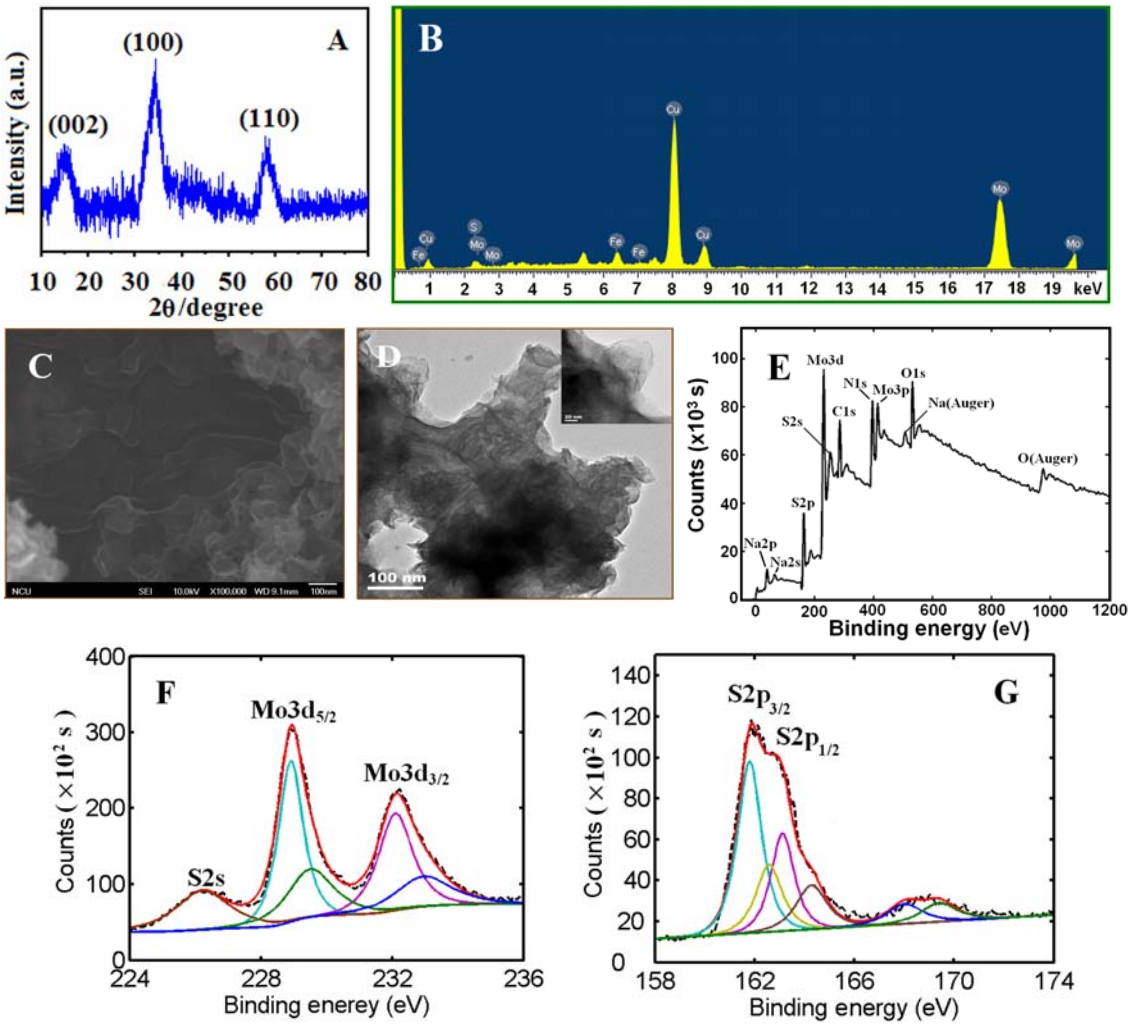

Figure 2

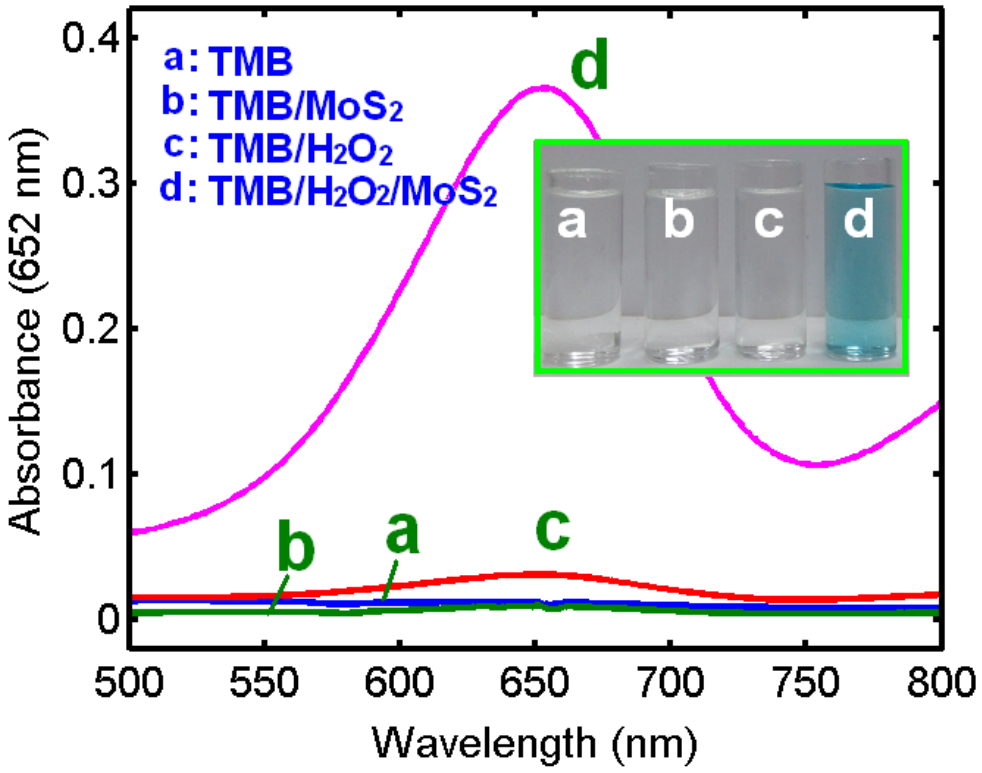

Figure 3

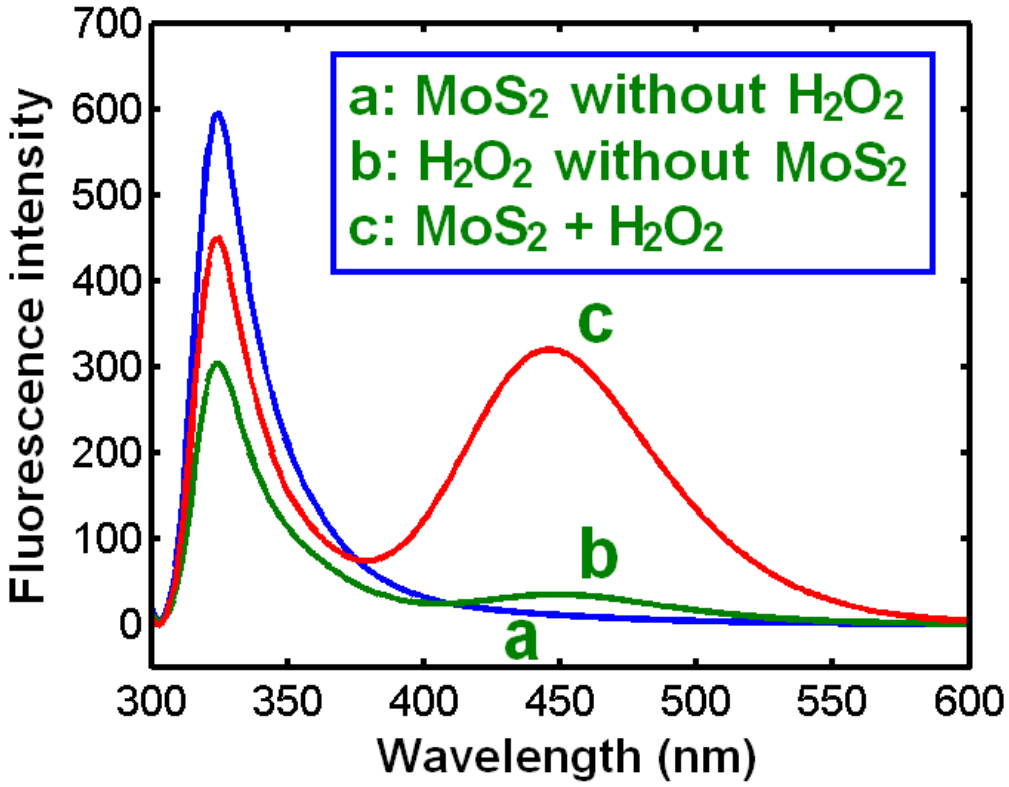

Figure 4

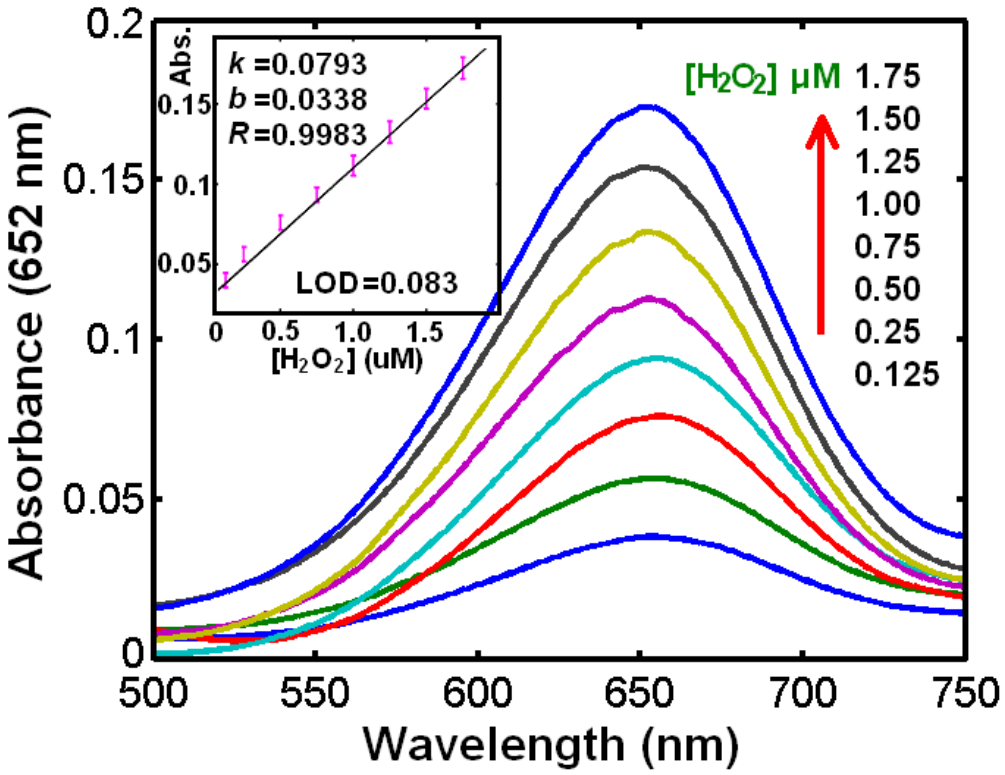

TOC (Table of contents)

Molybdenum disulfide (MoS_2) with a layered structure was synthesized and applied for trace analysis of H_2O_2 in water based on a colorimetric method.